JVI Journals.ASM.org

Lymph Node Macrophages Restrict Murine Cytomegalovirus Dissemination

Helen E. Farrell,[a] Nick Davis-Poynter,[a] Kimberley Bruce,[a] Clara Lawler,[a] Lars Dolken,[b] Michael Mach,[c] Philip G. Stevenson[a]

Sir Albert Sakzewski Virus Research Centre, School of Chemistry and Molecular Biosciences, University of Queensland and Royal Children's Hospital, Brisbane, Queensland, Australia[a]; Institut für Molekulare Infektionsbiologie, University of Würzburg, Würzburg, Germany[b]; Institut für Klinische und Molekulare Virologie, Friedrich-Alexander-Universität Erlangen-Nürnberg, Erlangen, Germany[c]

ABSTRACT

Cytomegaloviruses (CMVs) establish chronic infections that spread from a primary entry site to secondary vascular sites, such as the spleen, and then to tertiary shedding sites, such as the salivary glands. Human CMV (HCMV) is difficult to analyze, because its spread precedes clinical presentation. Murine CMV (MCMV) offers a tractable model. It is hypothesized to spread from peripheral sites via vascular endothelial cells and associated monocytes. However, viral luciferase imaging showed footpad-inoculated MCMV first reaching the popliteal lymph nodes (PLN). PLN colonization was rapid and further spread was slow, implying that LN infection can be a significant bottleneck. Most acutely infected PLN cells were CD169$^+$ subcapsular sinus macrophages (SSM). Replication-deficient MCMV also reached them, indicating direct infection. Many SSM expressed viral reporter genes, but few expressed lytic genes. SSM expressed CD11c, and MCMV with a cre-sensitive fluorochrome switch showed switched infected cells in PLN of CD11c-cre mice but yielded little switched virus. SSM depletion with liposomal clodronate or via a CD169-diphtheria toxin receptor transgene shifted infection to ER-TR7$^+$ stromal cells, increased virus production, and accelerated its spread to the spleen. Therefore, MCMV disseminated via LN, and SSM slowed this spread by shielding permissive fibroblasts and poorly supporting viral lytic replication.

IMPORTANCE

HCMV chronically infects most people, and it can cause congenital disability and harm the immunocompromised. A major goal of vaccination is to prevent systemic infection. How this is established is unclear. Restriction to humans makes HCMV difficult to analyze. We show that peripheral MCMV infection spreads via lymph nodes. Here, MCMV infected filtering macrophages, which supported virus replication poorly. When these macrophages were depleted, MCMV infected susceptible fibroblasts and spread faster. The capacity of filtering macrophages to limit MCMV spread argued that their infection is an important bottleneck in host colonization and might be a good vaccine target.

Human cytomegalovirus (HCMV) chronically infects more than 90% of the world's population. Latent virus is detectable in circulating monocytes; there also may be persistent stromal infection, and infectious virus is shed long term in secretions such as saliva (1). While most infections are asymptomatic, immune control can require substantial resources (2); immunocompromised patients suffer multiorgan disease, and HCMV is a leading cause of congenital disability. Therefore, better control would improve human health. So far, vaccines have failed to prevent infection or reduce long-term viral loads (3). One problem is that early infection events, which are key vaccine targets, remain ill defined. Virus behavior is cell type dependent, so an important unknown is which cell types HCMV infects first when colonizing new hosts.

Sporadic, asymptomatic HCMV transmission makes early infection hard to study (1). It is important to recognize, therefore, that HCMV is far from unique: CMVs colonize all mammals, and their species restrictions imply that this colonization predates most mammalian speciation. While virus-host pairs have since coevolved separately, even divergent viral genes often have equivalent functions in, for example, immune evasion (4), apoptosis suppression (5), and tropism switching (6). Therefore, a core CMV life cycle seems to be conserved. Consequently, animal CMVs can provide important information for understanding how HCMV works. Mice provide the main experimental model of mammalian biology, so MCMV (7) has particular value for defining how host and virus interact *in vivo*.

Natural MCMV entry routes remain ill defined. Transmission in breast milk is possible (8), but orally inoculated virus has not infected the neonatal gastrointestinal tract (9). MCMV can infect the lungs, but delivery here relies on inoculation under anesthesia (10) and needs further validation to qualify as natural entry. Most experimental infections have used intraperitoneal (i.p.) or intravenous (i.v.) virus inoculations, which seed rapidly to the liver and spleen (11) and probably also other sites. A monocyte-associated viremia follows (12), and MCMV spread to the salivary glands is monocyte dependent (13). Tracking floxed MCMV by recombination in cre transgenic mice shows that i.v. virions disseminate

Received 20 February 2015 **Accepted** 23 April 2015

Accepted manuscript posted online 29 April 2015

Citation Farrell HE, Davis-Poynter N, Bruce K, Lawler C, Dolken L, Mach M, Stevenson PG. 2015. Lymph node macrophages restrict murine cytomegalovirus dissemination. J Virol 89:7147–7158. doi:10.1128/JVI.00480-15.

Editor: K. Frueh

Address correspondence to Philip G. Stevenson, p.stevenson@uq.edu.au.

doi:10.1128/JVI.00480-15

via a TIE2$^+$ cell (14), possibly a vascular endothelial cell, and also possibly a radio-resistant myeloid cell (15).

While i.p. and i.v. inoculations have informed us about MCMV spread from vascular sites, they reach the blood directly and bypass the normal need to spread from a peripheral, primary site. Intrafootpad (i.f.) inoculations offer more scope to study this earlier phase of host colonization. Natural infections may not be subcutaneous, but i.f. inoculation allows controlled and reproducible virion delivery to a peripheral site. i.f. MCMV is hypothesized to enter the blood via vascular endothelial cells and patrolling monocytes (16). However, such infection has not been visualized directly, and the prediction that i.f. virus should seed rapidly to the spleen has not been tested. An alternative possibility is that i.f. MCMV reaches the blood via lymphatics. This would bring it into contact with popliteal lymph node (PLN) subcapsular sinus macrophages (SSM) (17). Several viruses have been tracked to SSM (18–20). SSM infection limits vesicular stomatitis virus (VSV) access to neurons, thereby reducing disease (19); however, VSV normally infects ungulates, so the physiological relevance of its behavior in murine SSM is unclear. In contrast, MCMV is a natural murine pathogen that exploits myeloid cells for dissemination. We established here how it spreads from the footpad.

MATERIALS AND METHODS

Mice. BALB/c, C57BL/6J, CD11c-Cre (21), and CD169-diphtheria toxin (DTx) receptor (DTR) mice (22) were maintained at University of Queensland animal units and used when they were 6 to 12 weeks old. Animal experiments were approved by the University of Queensland Animal Ethics Committee in accordance with Australian National Health and Medical Research Council (NHMRC) guidelines. Anesthesia was by isoflurane inhalation. Viruses were administered (10^6 PFU) either i.f. (50 μl) or i.p. (100 μl). For luciferase imaging, mice were given 2 mg D-luciferin i.p., anesthetized by isoflurane inhalation, and monitored for light emission by charge-coupled device camera scanning (Xenogen IVIS-200). To deplete phagocytic cells, mice were injected i.f. twice with 50 μl clodronate-loaded liposomes (http://clodronateliposomes.org/) (23) 3 to 5 days before infection. To deplete CD169$^+$ cells, CD169-DTR mice were injected i.p. twice with 100 ng diphtheria toxin (Sigma Chemical Co.) 1 to 3 days before infection. Depletion was essentially complete, as described previously (24). Mice were killed by exposure to a rising concentration of CO_2 or by cervical dislocation.

Cells and viruses. The detection of infected cells was facilitated by reporter viruses. For live imaging (MCMV-LUC), an HCMV IE1 promoter-driven luciferase expression cassette was inserted into m157 of a bacterial artificial chromosome (BAC)-cloned MCMV strain Smith genome that also was repaired for MCK2 expression (25). For fluorescent labeling of infected cells (MCMV-GR), an HCMV IE1 promoter-driven cassette was inserted into m157 of MCMV strain K181 by homologous recombination. This cassette, kindly provided by Alice McGovern (University of Queensland), encoded a floxed enhanced green fluorescent protein (EGFP) coding sequence upstream of nuclear-targeted tdTomato. Thus, exposure to cre switched viral fluorochrome expression irreversibly from EGFP to tdTomato. MCMV deleted of the essential virion glycoprotein L (gL) by inserting an HCMV IE1 promoter-driven LacZ cassette into M115 of strain K181 was propagated on gL-expressing NIH 3T3 cells (26). All other viruses were propagated on unmodified NIH 3T3 cells (American Type Culture Collection CRL-1658). Cells were grown in Dulbecco's modified Eagle's medium supplemented with 2 mM glutamine, 100 IU/ml penicillin, 100 μg/ml streptomycin, and 10% fetal calf serum. Virus was harvested from infected cells by low-speed centrifugation (500 × *g*, 10 min) to remove cell debris and then by ultracentrifugation (35,000 × *g*, 2 h).

Plaque assays. Infectious virus from cell culture or organ homogenates was quantified by plaque assay on murine embryonic fibroblasts (27). To detect gL-deficient MCMV, cells infected in the single round of replication were identified by fixation (1% formaldehyde, 30 min) and then incubation (2 h, 37°C) with 5-bromo-4-chloro-3-indolyl-β-D-galactopyranoside (1 mg/ml) in 100 mM sodium phosphate, pH 7.3, 1.3 mM magnesium chloride, 3 mM potassium ferricyanide, 3 mM potassium ferrocyanide (X-Gal).

Immunostaining. For immunofluorescence, organs were fixed in 1% formaldehyde–10 mM sodium periodate–75 mM L-lysine (24 h, 4°C), equilibrated in 30% sucrose (18 h, 4°C), and then frozen in OCT. Sections (6 μm) were air dried (1 h, 23°C), washed 3× in phosphate-buffered saline (PBS), blocked with 0.3% Triton X-100–5% normal goat serum (1 h, 23°C), and then incubated (18 h, 4°C) with combinations of primary antibodies (Ab) from anti-EGFP (rabbit polyclonal Ab [PAb]), anti-CD45R/B220 (rat monoclonal Ab [MAb] RA3-6B2), and F4/80 (rat MAb) (all from Santa Cruz Biotechnology); β-galactosidase (chicken PAb), CD11c (hamster MAb N418), ER-TR7 (rat MAb), and CD68 (rat MAb; FA-11) (all from AbCam); CD206 (rat MAb MR5D3) and CD169 (rat MAb 3D6.112) (from Serotec); and anti-MCMV (rabbit PAb raised by subcutaneous inoculation of rabbits with MCMV K181 propagated in NIH 3T3 cells). For CD11c staining, fixed sections first were treated with proteinase K (10 μg/ml; 5 min, 23°C). After incubation, sections were washed 3× in PBS, incubated (1 h, 23°C) with combinations of Alexa 568- or Alexa 647-conjugated goat anti-rat IgG PAb, Alexa 488- or Alexa 568-conjugated goat anti-rabbit IgG PAb (Life Technologies), Alexa 647-conjugated goat anti-hamster IgG PAb, and Alexa 488-conjugated goat anti-chicken IgG PAb (Abcam), and then washed 3× in PBS, counterstained with Hoechst 33342, and mounted in ProLong gold (Life Technologies). Fluorescence was visualized with a Zeiss LCM510 confocal microscope and analyzed with Zen imaging software. To detect β-galactosidase, organs were fixed and frozen as described above. Air-dried 6-μm sections were washed 3× in PBS and incubated with X-Gal (2 h, 37°C). Sections were counterstained with neutral red and mounted in VectaMount (Vector Laboratories).

Viral genome quantitation. DNA was extracted from organs or blood (NucleoSpin tissue kit; Macherey-Nagel). MCMV genomic coordinates 4166 to 4252 were amplified by PCR (LightCycler 480 SYBR green; Roche) and converted to genome copies by comparison with purified MCMV genomic DNA amplified in parallel. Cellular DNA was quantified in the same samples by PCR amplification of a β-actin gene fragment, again with template dilutions amplified in parallel. Viral DNA loads were normalized by cellular DNA loads.

Statistical analysis. Data were analyzed using GraphPad Prism 6.0. Experimental groups were compared by two-tailed Student's *t* test with Welch's correction; multiple groups within experiments were compared by two-way analysis of variance (ANOVA) test with Tukey's multiple comparison. Results with >95% confidence were considered significant.

RESULTS

Visualization of MCMV spread by luciferase expression. We used HCMV IE1 promoter-driven luciferase expression (MCMV-LUC) to track global MCMV spread after i.f. inoculation (Fig. 1). Live imaging (Fig. 1a and b) showed strong signals in the feet from day 1 and signals in the neck from day 6. Postmortem imaging of dissected organs (Fig. 1c and d) showed strong luciferase signals in footpads and the draining popliteal lymph nodes (PLN) from day 1. Luciferase signals were hard to detect in spleens until day 6. Neck signals were from the salivary glands. Occasional signals (approximately 1/5 mice) were observed in para-aortic LN from day 3 to day 6; none was observed in other LN or in the liver. Thus, i.f. MCMV rapidly reached the PLN, but several days passed before there was evidence of further, systemic spread. i.p. MCMV-LUC (Fig. 1e) showed luciferase signals mainly in the omentum at day 5 postinoculation but also in the spleen, indicating that the spleen could support early luciferase expression if virus reached it. There-

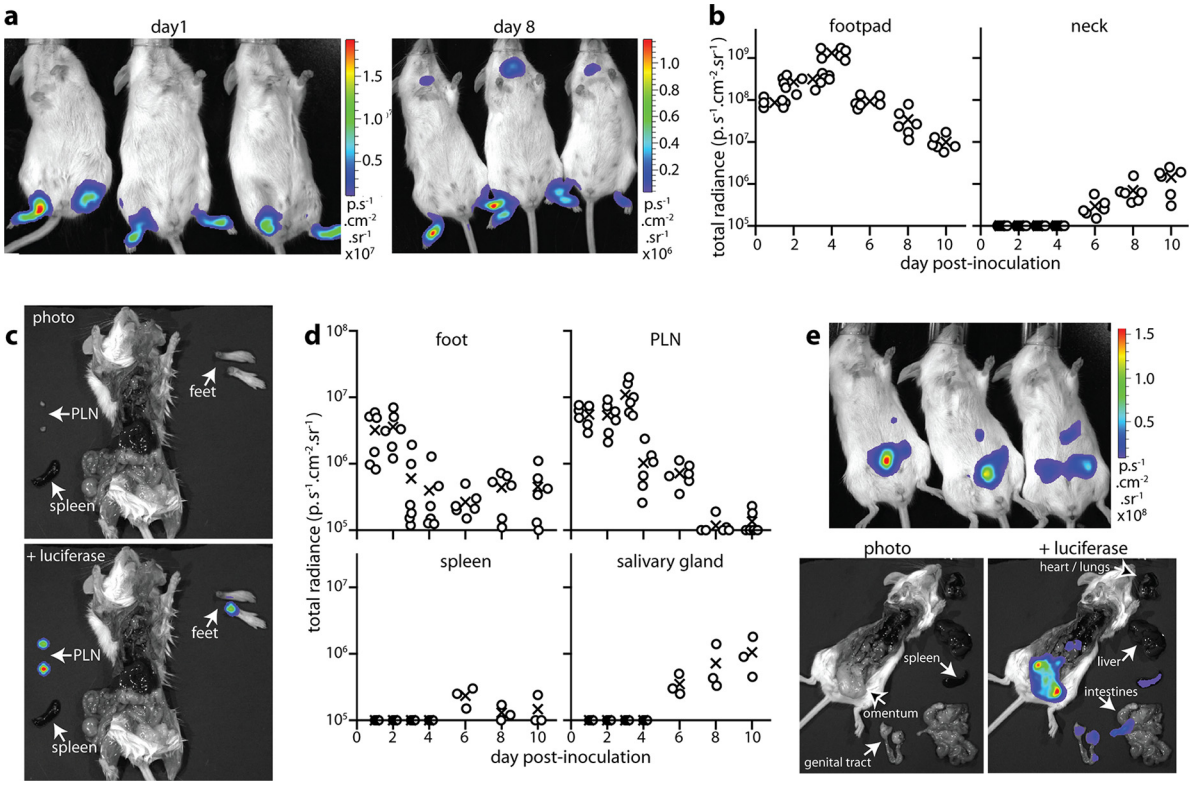

FIG 1 Visualizing MCMV spread by luciferase imaging. (a) BALB/c mice were given MCMV-LUC i.f. (10^5 PFU). Infection was tracked serially by i.p. luciferin injection and imaging light emission. Representative images are shown for days 1 (early infection) and 8 (after dissemination). (b) Mice were infected as described for panel a. Light emission (photons/second/square centimeter/steradian [$p.s^{-1}.cm^{-2}.sr^{1}$]) was quantitated by live imaging over 10 days. Circles show individuals, and crosses shows means. The baseline corresponds to the lower limit of assay sensitivity. (c) Mice were infected as described for panel a. Imaging after dissection was used to interpret live imaging signals. A representative image is shown for day 1 postinoculation. (d) Mice were infected as described for panel a. Signals in dissected organs were quantitated over 10 days (3 mice per time point). Circles show individuals, and crosses show means. The baseline corresponds to the lower limit of assay sensitivity. The neck signal came from the salivary glands. (e) BALB/c mice were infected i.p. with MCMV-LUC (10^5 PFU) and imaged after 5 days. Live imaging showed strong abdominal signals. Imaging after dissection showed that these signals came mainly from the omentum, but other intra-abdominal organs also were positive, including the spleen. Representative images are shown from 6 mice.

fore, the PLN were the proximate target for i.f. virions and seemed to restrict further, systemic spread.

Acute virus spread to PLN is not host or virus strain specific. Plaque assays of tissues from i.f. MCMV-LUC-inoculated BALB/c mice (Fig. 2a) showed high titers of infectious virus in footpads from day 1 and in PLN from day 2. Infectious virus was not detectable in spleens until day 3, and then only at low titers. Thus, plaque assays supported the conclusion from luciferase imaging that i.f. MCMV passes rapidly to the PLN and then slowly to the spleen and salivary glands. Negligible titers of infectious virus were recovered from blood. Quantitating viral DNA by PCR (Fig. 2b) showed a consistent picture: PLN DNA loads tracked those in footpads but were 10- to 100-fold lower; those in the spleen and the blood, while detectable above background, remained low. An equivalent i.p. inoculation gave 10- to 100-fold more viral DNA in blood (normalized by total DNA). Therefore, i.f. virus did not pass freely into the blood. Indeed, the lack of infectious virus in blood argued that much of the DNA detected here might have been infected cell debris rather than viable viral genomes.

MCMV-LUC was derived from MCK2-repaired strain Smith (28). Phenotypic differences are reported between Smith and the other main laboratory strain, K181 (29); in addition, mouse strains differ in susceptibility to MCMV infection (30). Therefore, to test the generality of our results, we analyzed by plaque assay the spread of i.f. K181 MCMV in C57BL/6 mice (Fig. 2c). The luciferase expression cassette of MCMV-LUC disrupted m157, which otherwise attenuates MCMV in Ly49H$^+$ mouse strains such as C57BL/6 (31). Therefore, our K181 MCMV also had an HCMV IE1-driven expression cassette in m157 (MCMV-GR). This encoded floxed EGFP upstream of tdTomato, so in mice lacking transgenic cre expression, as was the case here, MCMV-GR was EGFP$^+$ tdTomato$^-$. High titers of infectious virus were detected in footpads from day 1 postinoculation onwards, with peak titers at day 3. High titers of virus also were detected in PLN at days 1 and 3. As with MCMV-LUC, spleens did not yield infectious MCMV-GR until day 3. Therefore, PLN infection consistently preceded splenic infection, arguing that i.f.-inoculated MCMV spreads primarily via lymphatics.

***In situ* analysis of PLN infection.** PLN infection appeared to impose a delay on the spread of i.f.-inoculated MCMV. To understand better how this might work, we stained tissue sections for viral HCMV IE1 promoter-driven EGFP expression and cell type markers (Fig. 3a). The proportion all EGFP$^+$ PLN cells colocalizing with each marker was quantified across 5 to 12 fields of view for at least 3 mice (Fig. 3b). At day 1 postinoculation, EGFP was expressed predominantly in cells around the LN margins and co-

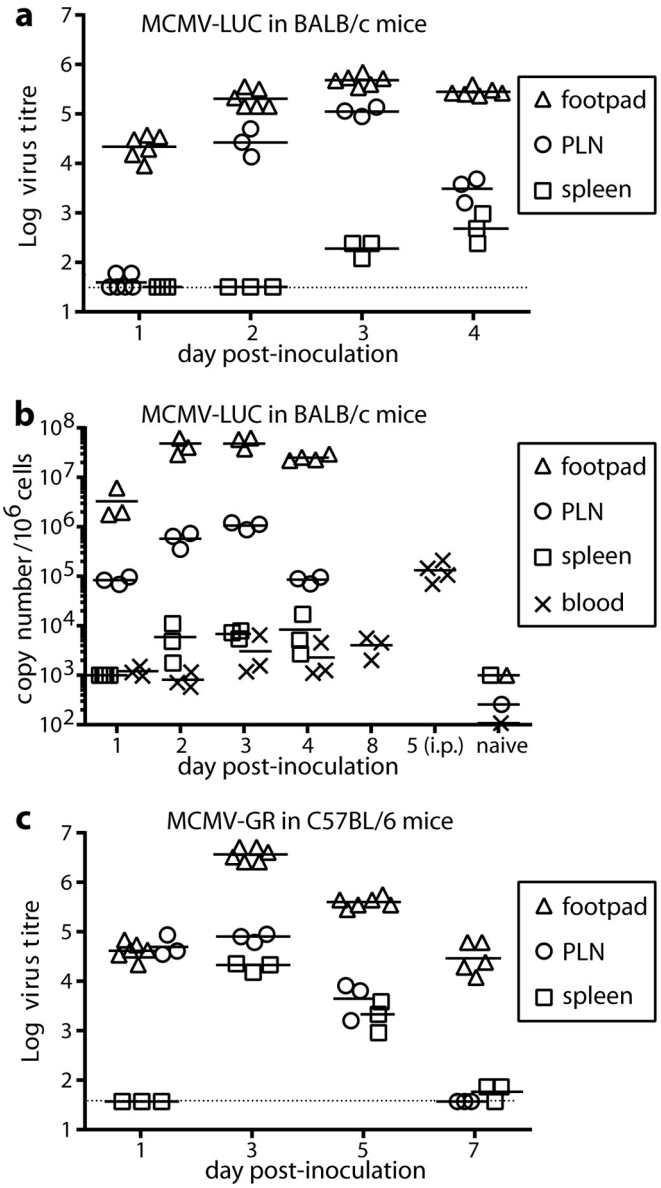

FIG 2 Kinetics of MCMV infectivity and DNA spread. (a) BALB/c mice were infected i.f. (10^5 PFU) with MCMV-LUC. Titers of infectious virus in organs were determined by plaque assay. Horizontal lines show means, and other symbols show individual mice. The dotted line shows the lower limit of assay sensitivity. Results shown are titers from spleens, PLN, and footpads on all days tested ($P < 0.0001$), except for spleens and PLN at day 1, when titers were very low. (b) Mice were infected as described for panel a. The viral DNA copy number was quantitated by PCR of extracted DNA as indicated. Horizontal lines show means, and other symbols show individual mice. Naive mice and day 5 i.p. infections (10^5 PFU) provided controls. Numbers of viral DNA copies were significantly higher in infected than in naive mice ($P < 0.001$), except for spleens on day 1 ($P > 0.05$). Numbers of viral DNA copies in blood were significantly higher in mice infected i.p. than at any time in mice infected i.f. ($P < 0.0001$). (c) C57BL/6 mice were infected i.f. (10^5 PFU) with MCMV-GR. Organs were plaque assayed as described for panel a. Horizontal lines show means, and other symbols show individual mice. The dotted line shows the lower limit of assay sensitivity. Titers were significantly lower in spleens than in PLN at days 1 and 3 ($P < 0.001$) and significantly lower than those of footpads on all days ($P < 0.0001$).

localized extensively with CD169 (sialoadhesin, Siglec-1). EGFP also showed colocalization with CD68 (an intracellular macrophage/granulocyte marker), CD206 (the mannose receptor), and F4/80 (a tissue macrophage marker) (32). There was little colocalization with the fibroblast marker ER-TR7 and none with B220 (B cells).

Myeloid populations are rarely uniform in glycoprotein expression, but generally SSM and medullary sinus macrophages (MSM) express CD169, while MSM and medullary cord macrophages (MCM) express F4/80 (17). MSM express more CD206 than do SSM. Therefore, the main infection target for i.f. MCMV in PLN was SSM. At day 3 postinoculation, viral EGFP expression remained mainly peripheral in the PLN, but there was a striking, general loss of CD169 expression that significantly reduced EGFP/CD169 colocalization. Colocalization with CD68, CD206, and F4/80 was preserved, and there was significantly more colocalization with ER-TR7. Thus, infection appeared to progress, albeit slowly, from SSM to PLN fibroblasts.

MCMV lytic antigen-positive cells were seen occasionally around the PLN margins but were much less evident than EGFP$^+$ cells (<10% total numbers) (Fig. 3c). This was consistent with HCMV IE1-driven cassettes operating independently of the viral lytic cycle (33) and argued that most MCMV-infected PLN cells were not lytically infected. This agreed with PLN showing HCMV IE1 promoter-driven luciferase signals similar to those of footpads (Fig. 1) but yielding 10- to 100-fold fewer PFU (Fig. 2).

Staining infected lung sections established the efficacy of the immune serum in detecting lytic infection (Fig. 3c). New lytic antigen staining occurred in PLN as a pan-cellular distribution (Fig. 3c, arrow). More PLN cells showed lytic antigens in a subcellular distribution. This presumably reflected virions and infected cell debris from the footpads being trapped by SSM without new lytic infection. Thus, some of the PFU recovered from PLN possibly were virions arriving from the footpads rather than being produced in the PLN. This did not change our conclusion that MCMV spreads via LN but suggested that the restriction of virus replication in PLN was more marked than was revealed by plaque assays.

MCMV SSM infection is direct. To determine whether SSM were direct infection targets, we used i.f. virions in which HCMV IE1 promoter-driven β-galactosidase (β-gal) disrupts the coding sequence of an essential virion component, glycoprotein L (gL) (34). The virions were pseudotyped gL$^+$ by growth in complementing cells and were infectious and could make new virions, but a lack of gL rendered any new virions noninfectious. Thus, infection was restricted to the first cells encountered. Immunostaining for β-gal (Fig. 4a and b) showed infection around the PLN margin that colocalized mainly with CD169 and CD68. Lytic antigens, from either input virions passing along the lymphatics or the single gL$^-$ replication cycle, also were visible around the subcapsular sinus (Fig. 4a). The similar distributions of gL$^+$ and gL$^-$ infections supported the idea that replication-competent MCMV spreads poorly within the PLN.

At 6 h postinoculation, infectious gL$^-$ MCMV could be recovered from both footpads and PLN (Fig. 4c), implying a direct passage of inoculated virions to the PLN. At 24 h postinoculation, infectious gL$^-$ MCMV was detected only in footpads. In contrast, gL$^+$ PLN titers increased from 6 h to 24 h postinoculation, consistent with virus replication. However, this did not necessarily occur in the PLN, as footpad plaque titers also increased and were

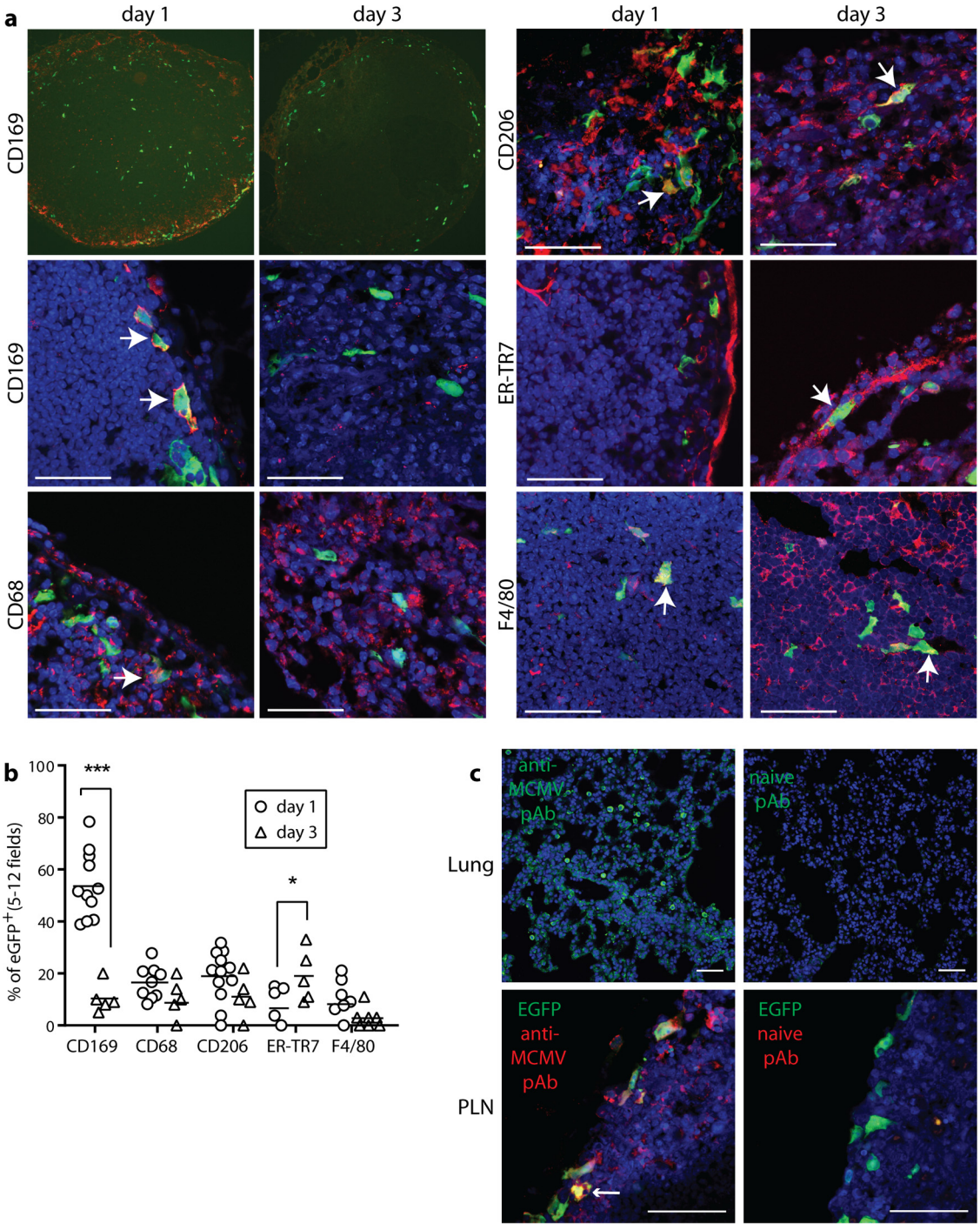

FIG 3 *In situ* analysis of PLN infection after i.f. MCMV. (a) C57BL/6 mice were given MCMV-GR i.f. (10^6 PFU). PLN taken 1 or 3 days later were stained for viral EGFP (green) and cell type markers as indicated (red). Arrows show examples of colocalization. Nuclei were stained with Hoechst 33342 (blue). Scale bars show 50 μm. The upper left panels show whole-PLN overviews, with nuclear staining omitted for clarity, showing loss of CD169 staining at day 3. (b) Quantitation of colocalization for which panel a shows examples. Five to 12 fields of view were examined from at least 3 separate PLN. From day 1 to day 3, the proportion of $EGFP^+$ cells that were $CD169^+$ decreased significantly (***, $P < 0.001$), and the proportion that were $ER\text{-}TR7^+$ increased significantly (*, $P < 0.05$). (c, upper) Lung sections of C57BL/6 mice 3 days after MCMV-GR inhalation. (Lower) PLN on day 1 of infection with fewer lytic $antigen^+$ cells (red) than $EGFP^+$ cells (green) (<10% total numbers). The arrow shows an example of colocalization (an $EGFP^+$ lytically infected cell).

10- to 100-fold higher than PLN titers. The gL^- viral DNA load in PLN did not decline from 6 h to 24 h (Fig. 4d), presumably because gL^- MCMV produces new (noninfectious) virions. Both gL^- and gL^+ viral DNA loads in blood were low at 6 h and 24 h. The gL^- input (6 h) appeared to be higher, but only gL^+ DNA loads increased from 6 h to 24 h. Viral DNA loads were consistently at least 100-fold lower in blood than in the PLN, and there was negligible infectious virus in blood.

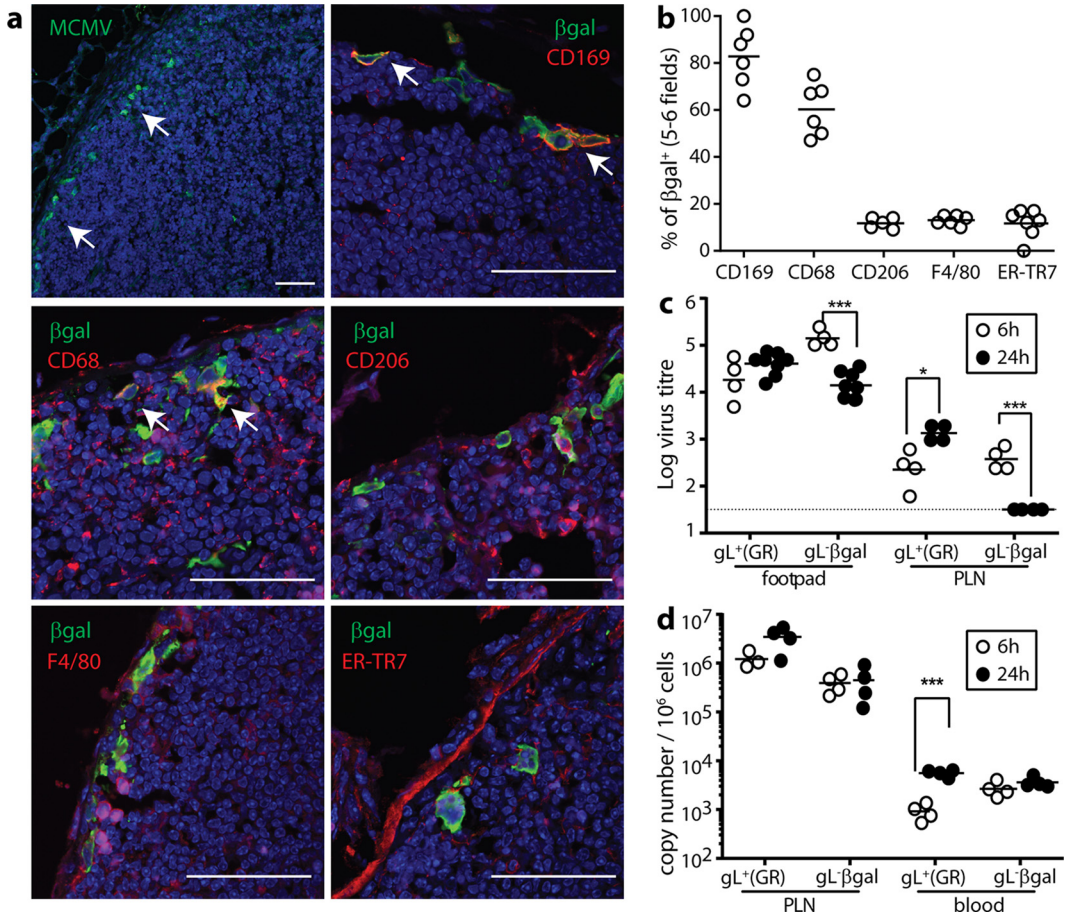

FIG 4 Direct infection of SSM. (a) C57BL/6 mice were infected i.f. with MCMV in which a β-galactosidase expression cassette disrupts gL (gL$^-$βgal) (10^6 PFU). PLN harvested 24 h later were stained for lytic antigens (MCMV) or β-gal to identify infection (green) and for cell type-specific markers to localize it (red). Nuclei were stained with Hoechst 33342. Arrows show examples of colocalization. Scale bars show 50 μm. (b) Colocalization, as illustrated in panel a, was quantitated across 5 to 7 fields of view from PLN of 3 mice. Circles show individual counts, and horizontal lines show means. (c) C57BL/6 mice were infected i.f. with either gL$^-$ β-gal MCMV or gL$^+$ MCMV-GR as a control (10^6 PFU). Titers of infectious virus in organs were determined by plaque assay 6 or 24 h later. Circles show individual mice, and horizontal lines show means. Preformed infectious gL$^-$ β-gal MCMV was detectable at 6 h, but titers then fell significantly from 6 to 24 h (***, $P < 0.001$). MCMV-GR titers in PLN increased significantly over the same period (*, $P < 0.05$). The dotted line shows the limit of assay detection. (d) Mice were infected as described for panel c, and viral DNA loads were quantitated by PCR. gL$^-$ β-gal DNA loads were maintained. All DNA loads in blood were low, but those of MCMV-GR increased significantly from 6 to 24 h (***, $P < 0.001$). The baseline corresponds to the lower limit of assay detection.

SSMs provide a functional barrier to MCMV spread. To test functionally the contribution of SSM to MCMV host colonization, we depleted them by injecting i.f. clodronate-loaded liposomes 3 to 5 days before MCMV-LUC. This had little effect on MCMV-LUC infection, as judged by live imaging (Fig. 5a). Imaging dissected tissues (Fig. 5b) similarly showed little effect of clodronate on the colonization of footpads or PLN. However, spleen colonization increased significantly. Viral DNA loads in the blood also increased (Fig. 5c).

We next tracked the effects of clodronate treatment on C57BL/6 mouse colonization by gL$^+$ (MCMV-GR) and gL$^-$ viruses. For MCMV-GR (Fig. 6a), plaque assays showed an increase in footpad, PLN, and spleen colonization, with the greatest increase (>100-fold) in PLN. Viral DNA loads in the blood also increased (Fig. 6b), consistent with the results for MCMV-LUC (Fig. 5b). The increase in MCMV-GR plaque titers in PLN at 1 day postinoculation, without a corresponding increase in MCMV-LUC luciferase signals (Fig. 5b), suggested that in clodronate-treated mice PLN infection was more lytic, as luciferase expression was from a lytic cycle-independent promoter. Consistent with this idea, *in situ* analysis of MCMV-GR infection (Fig. 6c) showed no significant change in the total number of cells expressing HCMV IE1 promoter-driven EGFP$^+$. However, the distribution of EGFP expression changed, from around the subcapsular sinus to nearer PLN follicles, as defined by B220 staining. Clodronate treatment depleted CD169$^+$ cells from the subcapsular sinus, so EGFP/CD169 colocalization was lost. MCMV antigen$^+$ cells were more numerous, and, like EGFP$^+$ cells, were seen further within the LN substance. Here, ER-TR7 staining was increased, with a less ordered distribution than that in control infected PLN, where it was confined largely to the subcapsular sinus. EGFP$^+$ cells were closely associated with the abnormal ER-TR7 staining, suggesting that in clodronate-treated mice, MCMV infected PLN fibroblasts. Costaining for ER-TR7, EGFP, and lytic antigens (Fig. 6d) revealed that many of the EGFP$^+$ fibroblasts were lytically infected.

X-Gal staining (based on HCMV IE1 promoter-driven viral β-gal) showed a similar penetration into the PLN of replication-

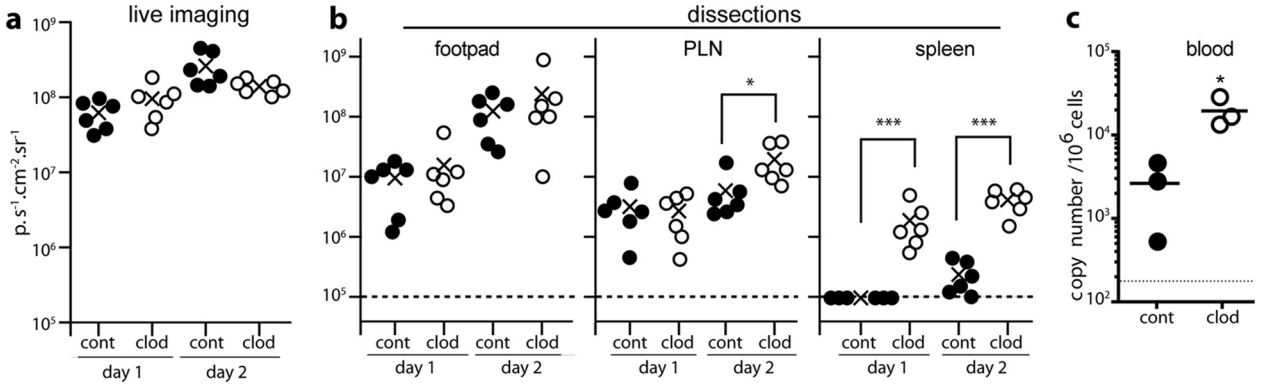

FIG 5 SSM depletion increases MCMV dissemination. (a) BALB/c mice were injected i.f. with clodronate-loaded liposomes (clod), or were left untreated (cont), at 5 and 3 days prior to i.f. inoculation with MCMV-LUC (10^5 PFU). Mice were imaged for light emission 1 and 2 days later. Circles show individuals, and crosses show means. No significant difference was observed between clodronate-treated and untreated mice ($P > 0.05$). (b) Mice infected as described for panel a were dissected for imaging of individual organs. Clodronate has no significant effect on footpad infection but increased PLN infection at day 2 ($P < 0.05$) and increased spleen infection at both time points ($P < 0.001$). Dashed lines show the lower limit of assay sensitivity. (c) Mice were left untreated or were treated with clodronate liposomes and infected as described for panel a, and viral DNA was quantitated in blood by PCR 1 day later. Circles show individual mice, and horizontal lines show means. Clodronate treatment significantly increased viral DNA loads in blood ($P < 0.05$).

deficient (gL$^-$) MCMV after clodronate treatment (Fig. 6e). One hundredfold more gL$^-$-infected cells (X-Gal$^+$) were detected in the spleens of clodronate-treated mice, indicating that SSM depletion also allowed direct viral spread from footpad to spleen. Therefore, by virion capture from the afferent lymph, SSM restricted the spread of i.f. MCMV into the PLN and the blood. The spread of gL$^-$ MCMV argued that without this capture, virions simply flow along LN channels to the efferent lymphatics.

CD169$^+$ cell depletion confirms the importance of SSM in MCMV containment. Clodronate-loaded liposomes deplete phagocytic cells generally rather than just SSM and can affect B cell responses (35). Therefore, to confirm the importance of SSM for containing i.f. MCMV, we depleted CD169$^+$ by diphtheria toxin (DTx) treatment of CD169-DTx receptor (DTR) transgenic mice (22) (Fig. 7). Again, virus loads increased: plaque assays at day 1 postinoculation showed modest increases in footpad and PLN titers and a marked increase in splenic titers. (DTx depletes cells much more rapidly than do clodronate-loaded liposomes, so we could look earlier in infection, before virus replication built up high titers in the PLN.) Thus, in the absence of CD169$^+$ cells, MCMV passed rapidly from footpad to spleen. DTx may have increased splenic viral loads more than liposomal clodronate did, because it also depletes CD169$^+$ splenic metallophilic marginal-zone macrophages (MZM), whereas i.f. clodronate does not (23). Nonetheless, increased splenic infection established that the PLN infection bottleneck was CD169$^+$ cell dependent, consistent with a key role for SSM.

Genetic tagging shows little MCMV replication in CD11c$^+$ cells. The limited MCMV lytic antigen expression of SSM argued that their infection is poorly productive. As a more direct measure of virus production in myeloid cells, we infected CD11c-cre mice (21) with MCMV-GR. Cre recombinase switches MCMV-GR from green (EGFP) to nuclear-targeted red (tdTomato) fluorochrome expression, and SSM express CD11c, as they are depleted by DTx in CD11c-DTR mice (36). We depleted mice of SSM with i.f. liposomal clodronate before infection with MCMV-GR. After 1 day, the virus recovered from PLN and spleens was unswitched, regardless of clodronate treatment (Fig. 8a).

Immunostaining PLN sections showed that up to 40% of fluorescent cells in undepleted, infected mice expressed nuclear tdTomato (Fig. 8b, control). This was consistent with SSM expressing CD11c and argued further that SSM infection produced few new virions. Most tdTomato$^+$ CD169$^+$ cells around the subcapsular sinus also were EGFP$^+$ (Fig. 8b, upper, control, large arrows), implying delayed or incomplete switching of infecting genomes. Fully switched infected cells (EGFP$^-$ tdTomato$^+$; small arrows) were deeper in the PLN and CD169$^-$ cells, consistent with MCMV also infecting CD11c^{hi} dendritic cells. The lack of switched progeny virions (Fig. 8a) argued that this infection also was poorly productive. Some viral lytic antigen staining (Fig. 8b, lower, control) was associated with the part-switched cells around the subcapsular sinus (large arrows). None was associated with the fully switched cells (small arrows). Thus, CD11c^{hi} dendritic cells seemed to switch viral genomes more efficiently than CD11c^{lo} SSM in CD11c-cre mice, but neither cell type contributed significantly to new virus production. (Because fluorochrome expression was from a lytic cycle-independent promoter, cells could be fluorescent without lytic infection.)

In mice treated with clodronate-loaded liposomes before i.f. MCMV-GR (Fig. 8b, clodronate), CD169 expression was lost, EGFP$^+$ cells appeared deeper within the PLN than the subcapsular sinus, and essentially all of these cells were EGFP$^+$ tdTomato$^-$. Thus, infection shifted to a CD11c$^-$ cell, whereas results shown in Fig. 6 indicate a shift to a fibroblast. Many of the EGFP$^+$ cells expressed MCMV lytic antigens (Fig. 8b, lower, clodronate). Dendritic cells resist depletion by clodronate-loaded liposomes because they are poorly phagocytic (23). However, they receive antigens from SSM (18), and herpesviruses exploit immune communication pathways to spread (37), so the loss of tdTomato$^+$ cells in PLN of clodronate-treated mice possibly reflected that MCMV reaches dendritic cells via SSM.

As control infected mice showed substantial MCMV-GR switching *in situ* on PLN sections at day 1 postinoculation (Fig. 8b), we assayed their subsequent production of switched infectious virus at day 3 (Fig. 8c). Virus titers were substantially higher than they were at day 1, but switched virus remained <1% of the

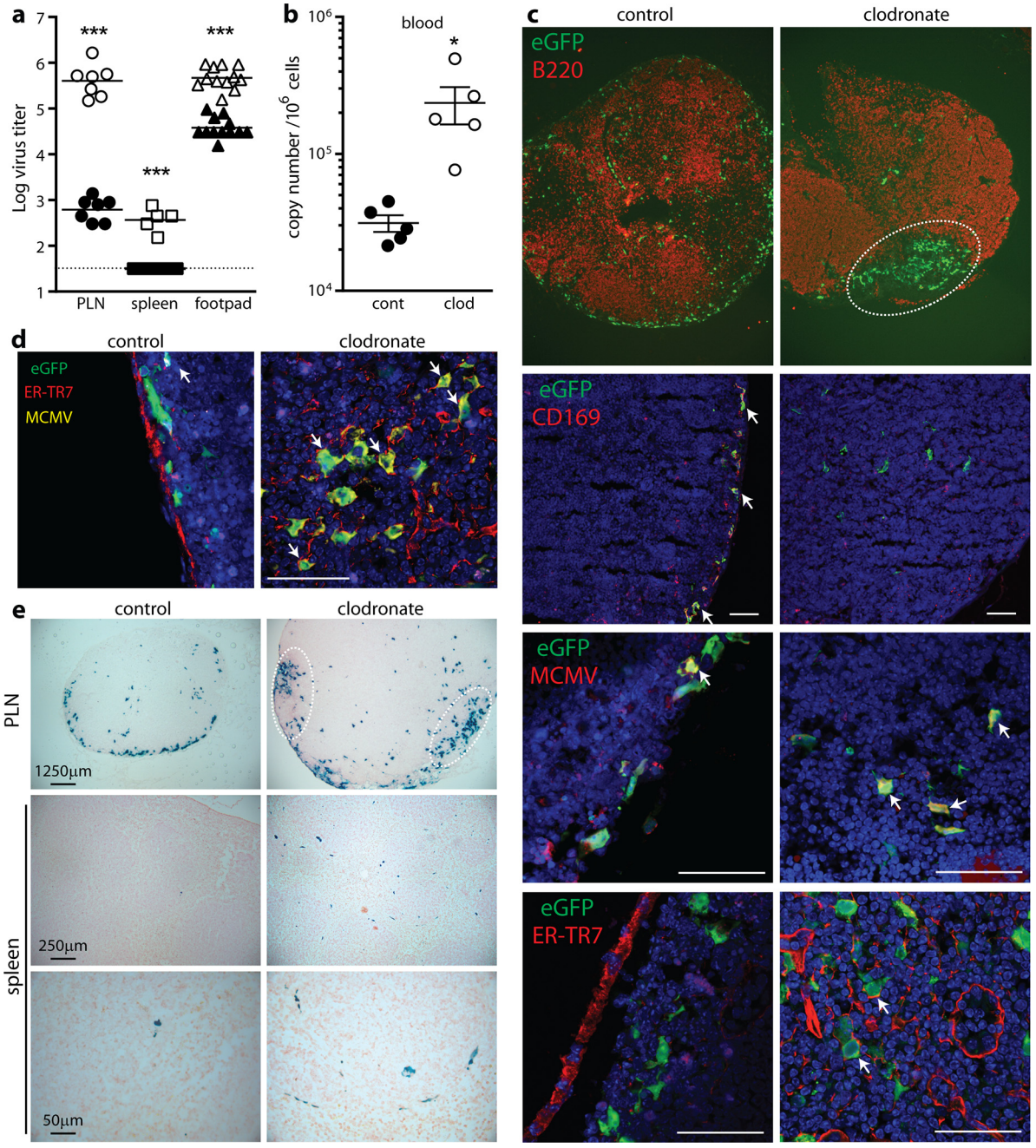

FIG 6 SSM depletion alters MCMV distribution in the PLN. (a) C57BL/6 mice were left untreated (closed symbols) or were given clodronate-loaded liposomes i.f. 5 and 3 days before i.f. infection with MCMV-GR (10^6 PFU). One day later, footpads ($n = 12$), PLN ($n = 7$), spleens ($n = 5$), and blood ($n = 5$) were harvested and plaque assayed for infectious virus. Horizontal lines show means, and other symbols show individual mice. The dotted line shows the lower limit of virus detection. Clodronate treatment significantly increased virus titers in footpads, PLN, and spleens (***, $P < 0.001$). (b) Mice were given liposomal clodronate i.f. (clod) or were left untreated (cont), and then they were infected with MCMV-GR as described for panel a. One day later, viral DNA loads in blood were quantitated by PCR. Clodronate treatment significantly increased the viral DNA load (*, $P < 0.05$). (c) Mice were treated with clodronate or left untreated and infected with MCMV-GR as described for panel a. PLN sections were stained for virus-expressed EGFP (green) and cell type markers or viral lytic antigens (MCMV) (red). Nuclei were stained with Hoechst 33342. (Top) Low-power images without nuclear staining show the overall distribution of EGFP, with an area of deeper penetration in clodronate-treated mice outlined. Arrows in the higher-power images show examples of colocalization. Scale bars show 50 μm. Clodronate treatment depleted $CD169^+$ cells from the subcapsular sinus and led to viral EGFP colocalizing with the fibroblast marker ER-TR7. (d) Mice were left untreated or were treated with clodronate and infected with MCMV-GR as described for panel a. PLN sections were stained for virus-expressed EGFP (green), viral lytic antigens (MCMV) (yellow), and the fibroblast marker ER-TR7 (red). Nuclei were stained with Hoechst 33342. Arrows show examples of lytically infected fibroblasts, which were much more numerous after clodronate treatment (>5-fold increase). (e) C57BL/6 mice were depleted of clodronate or left untreated, as described for panel a, and then infected i.f. with replication-deficient gL^-β-gal MCMV. Virus infection on tissue sections was revealed by X-Gal staining. Infection again penetrated deeper into the PLN cortex after clodronate treatment (regions outlined). Spleens also showed significantly more infected cells (20.3 ± 12.1 per low-power field and 0.3 ± 0.1 for untreated controls [means ± SEM, $n = 6$]) ($P < 0.001$).

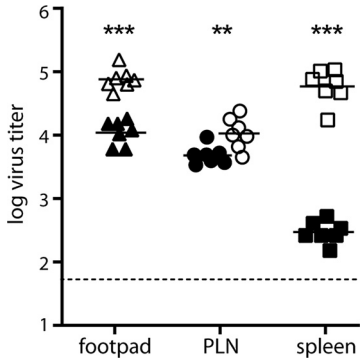

FIG 7 CD169$^+$ cell depletion promotes MCMV spread. CD169-DTR mice were left untreated (closed symbols) or were given diphtheria toxin i.p. (open symbols) at 3 and 1 days before i.f. infection with MCMV-GR (10^6 PFU). Two days later, organs were plaque assayed for infectious virus. Horizontal lines show means, and other symbols show individual mice. The dashed line shows the limit of virus detection. Clodronate treatment significantly increased the virus titers in PLN (**, $P < 0.01$), footpads, and spleens (***, $P < 0.001$). The dotted line shows the limit of assay sensitivity.

total in all sites. Therefore, CD11c$^+$ cells, which included SSM, poorly supported MCMV replication. Staining LN infected for 1 day confirmed that CD169$^+$ cells express CD11c (Fig. 8d) and showed virus-expressed EGFP in both CD11c$^+$ CD169$^+$ and CD11c$^+$ CD169$^-$ cells (Fig. 8e), but infection of neither cell subset contributed significantly to infection reaching the spleen.

DISCUSSION

Most analyses of host colonization by MCMV have used i.p. or i.v. inoculations. These deliver virions directly to the blood. How MCMV (or HCMV) first reaches the blood from peripheral sites has been unclear. i.f.-inoculated MCMV spread via draining LN. We saw no evidence of direct vascular spread bypassing LN infection. Inoculating replication-deficient MCMV established SSM as a direct infection target. CMVs classically replicate in differentiated myeloid cells (38), but SSM allowed little viral replication, and their depletion increased acute infection spread. This increase was associated with an infection of stromal cells rather than other myeloid cells. Thus, SSM infection constituted a significant bottleneck in MCMV dissemination after i.f. inoculation.

MCMV spread conformed essentially to the model established for ectromelia virus (39): peripheral infection, primary viremia, myeloid infection, secondary viremia, and then dissemination to tertiary shedding sites. i.p. and i.v. MCMV inoculations directly establish a primary viremia. After i.f. inoculation, LN infection intervened. Within PLN, MCMV capture by SSM paralleled a similar capture of i.f.-inoculated viruses that have not evolved to colonize mice (18–20). Such convergence of spread between unadapted and host-adapted viruses reflects that the routes are set at least as much by the host as by viral functions. Antigens from most tissues reach the blood via LN, so this is the main route taken by viruses whose tropism promotes systemic spread.

LN both prime adaptive immunity and function as protective filters to stop pathogens from reaching the blood. SSM were not wholly effective filters; nonetheless, they substantially slowed the spread of i.f.-inoculated MCMV by poorly supporting productive infection and by restricting access to permissive fibroblasts. Fibroblasts were infected to a degree in the presence of SSM, but they were infected much more readily and apparently lytically when SSM were depleted. Limited switched virus production in CD11c-cre mice, despite *in situ* evidence of switching in SSM and dendritic cells, argued that fibroblasts are the main LN site of MCMV replication.

Myeloid cells generally do not enter efferent lymphatics (40), and LN myeloid cells presumably die *in situ* after antigen presentation. Therefore, MCMV may spread from LN as cell-free virions rather than in myeloid cells. The contrasting, myeloid-associated viremia of i.p. MCMV (13) could result from virions directly reaching monocyte precursors in the bone marrow or from infected peritoneal macrophages entering the thoracic duct. Cell-free virions can exit the circulation via sinusoidal capillaries. These occur in the spleen, bone marrow, salivary glands, liver, LNs, adrenals, and pancreas. Therefore, an early, cell-free viremia could infect these sites before bone marrow-derived monocytes become the main means of virus spread. Murid herpesvirus 4 (MuHV-4) similarly establishes a cell-free primary viremia after seeding to and then replicating in LN (37). However, CD11c$^+$ cell infection (41) plays a more prominent role in LN infection than it did with MCMV, and in the long term MuHV-4 disseminates primarily via infected B cells (42).

The containment of i.f.-inoculated MCMV by SSM paralleled the containment of systemically inoculated MCMV by splenic MZM (43, 44), consistent with SSM and MZM analogously filtering the afferent lymph and blood. MCMV containment by SSM further paralleled their containment of i.f. VSV (45). That SSM and MZM generally restrict virus spread suggests a generic defense mechanism. SSM were infected within 6 h of MCMV inoculation, so this was unlikely to be adaptive immunity; rather, the delay imposed by SSM allowed time for adaptive priming to occur. NK cells help to control MCMV replication in SSM (46), but they are not immediately effective (47), and while NK cells restrict m157$^+$ MCMV spread in C57BL/6 mice (30), SSM limited m157$^-$ virus spread in both BALB/c and C57BL/6 mice. Thus, an intrinsic mechanism seemed more likely, as proposed for MZM restricting i.p. MCMV (44).

The alpha/beta interferons (IFN) are one candidate, as SSM prominently express IFN in response to viral infection (48), and IFN can restrict MCMV spread *in vivo* (49–51). High MZM expression of USP18, which negatively regulates the IFN-dependent effector ISG15 (52), may reflect a cytoprotective adaptation to strong IFN responses (53) in cells abundantly exposed to incoming viruses; widespread loss of CD169 expression 3 days after i.f. MCMV, when viral lytic replication was far from extensive, suggested a host response, such as IFN-dependent apoptosis, rather than a direct viral effect, and the failure of SSM to restrict MCMV replication completely perhaps reflected viral IFN evasion. However, other mechanisms are equally possible, so this requires further investigation. Although HCMV lytic reactivation can be induced *in vitro* by monocyte differentiation (38), the poor lytic replication of MCMV in SSM and LN dendritic cells implied that *in vivo*, other factors also are important. The capacity of SSM to restrict the spread of i.f.-inoculated MCMV suggested that mucosally inoculated MCMV bypass SSM. Dendritic cells, which can migrate between SSM (54) and disseminate MuHV-4 (41), seemed not to disseminate MCMV, but migratory CD11c$^-$ myeloid cells are a possible means of transport. The present data establish that for i.f.-inoculated MCMV, spread occurs via LN and SSM are a direct and rate-limiting infection target.

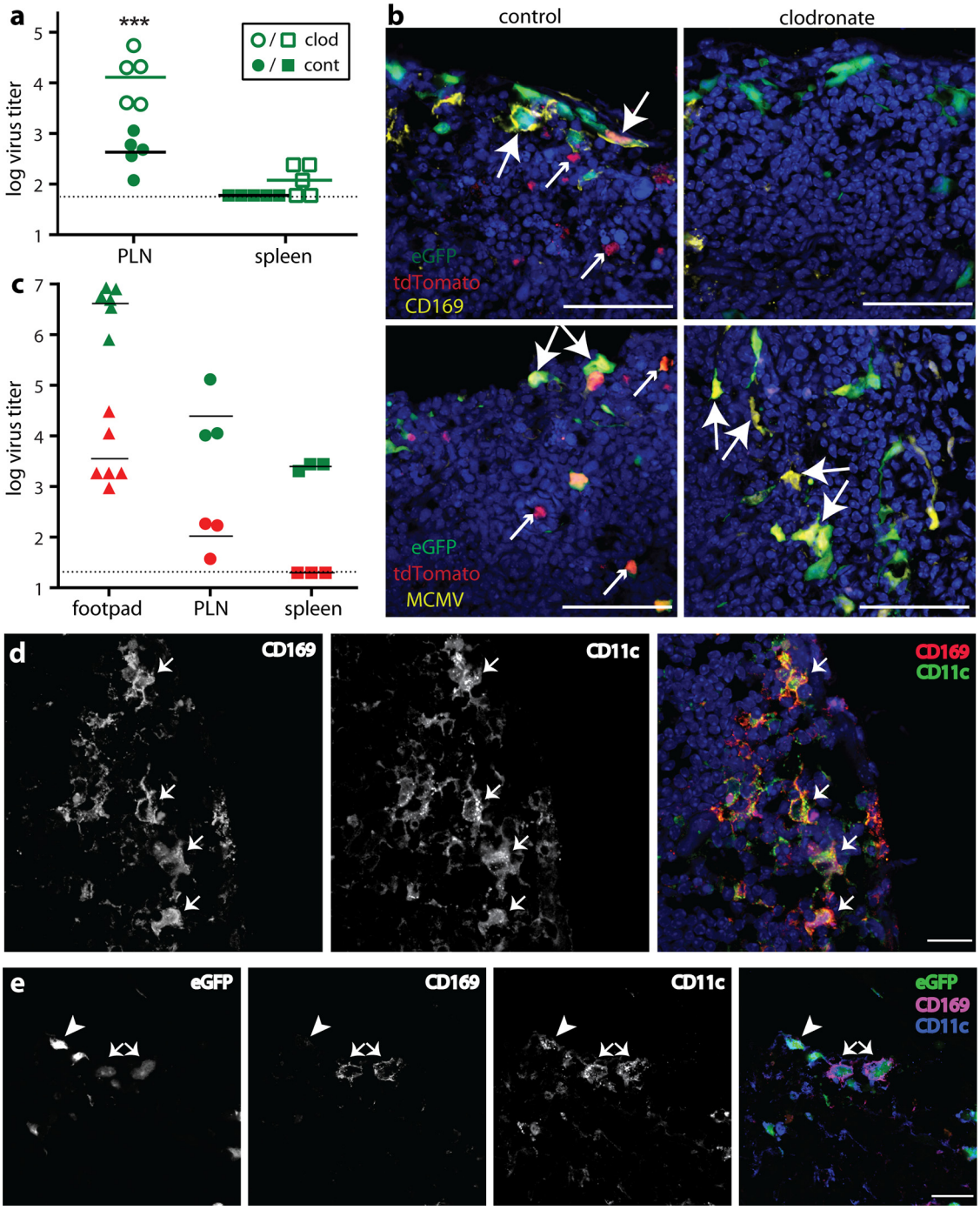

FIG 8 Viral fluorochrome switching reveals MCMV infection of CD11c$^+$ cells but little evidence of MCMV replication. (a) CD11c-cre mice were depleted of SSM by i.f. injection of clodronate-loaded liposomes (clod) or were left untreated (cont), and then all mice were infected i.f. with MCMV-GR (10^6 PFU). PLN and spleens harvested 1 day later were plaque assayed for EGFP$^+$ and tdTomato$^+$ virus. Only unswitched (EGFP$^+$) virus was detected. Horizontal lines show means. Other symbols show individual mice. The dotted line shows the limit of assay sensitivity. Clodronate treatment significantly increased (unswitched) virus titers in PLN (***, $P < 0.001$). (b) CD11c-cre mice were left untreated (control) or were depleted of SSM by i.f. liposomal clodronate 5 and 3 days before i.f. MCMV-GR inoculation (10^6 PFU). PLN harvested 3 days later were stained for EGFP (green), tdTomato (red), and CD169 or MCMV lytic antigens (MCMV) (yellow). In the upper control panel, large arrows show CD169$^+$ cells around the subcapsular sinus that express both EGFP and nuclear tdTomato (partially switched). Small arrows show completely switched cells that are CD169$^-$. Clodronate treatment removed CD169 staining from the subcapsular sinus. Cells just below the sinus became infected and were unswitched. Lytic antigen staining was seen around the subcapsular sinus in control mice (lower panel, large arrows) and was associated with partial switching. Completely switched cells showed no lytic antigen staining (small arrows). After clodronate treatment, lytic antigen staining was seen further into the PLN cortex in cells infected with unswitched virus. Scale bars show 50 μm. (c) CD11c-cre mice were infected i.f. with MCMV-GR (10^6 PFU). Footpads, PLN, and spleens harvested 3 days later were plaque assayed for EGFP$^+$ (green) and tdTomato$^+$ (red) viruses. Horizontal lines show mean titers for each. Other symbols show individual mice. Switched virus (red) accounted consistently for <1% of the total. The dotted line shows the limit of assay sensitivity. (d) C57BL/6 mice were infected i.f. with gL$^-$ MCMV (10^6 PFU). PLN harvested 2 days later were stained for CD169 (red in the merged image) and CD11c (green in the merged image). Nuclei were stained with Hoechst 33342 (blue). Scale bars, 20 μm. Arrows show examples of colocalization (CD169$^+$ CD11c$^+$ SSM). (e) C57BL/6 mice were infected i.f. with MCMV-GR (10^6 PFU). PLN harvested 2 days later were stained for CD169 (cyan in the merged image), CD11c (blue in the merged image), and viral EGFP (green in the merged image). Viral EGFP is seen in a CD11c$^+$ CD169$^-$ dendritic cell (large arrowhead) and CD11c$^+$ CD169$^+$ SSM (small arrows).

ACKNOWLEDGMENTS

This work was supported by grants from the Australian Research Council (FT130100138), National Health and Medical Research Council (project grants 1064015, 1060138, and 1079180), and Belspo (BelVir).

We thank Ulrich Koszinowski for making freely available the BAC-cloned MCMV strain Smith genome and Alice McGovern for providing reagents.

REFERENCES

1. **Britt W.** 2007. Chapter 41. Virus entry into host, establishment of infection, spread in host, mechanisms of tissue damage. *In* Arvin A, Campadelli-Fiume G, Mocarski E, Moore PS, Roizman B, Whitley R, Yamanishi K (ed), Human herpesviruses: biology, therapy, and immunoprophylaxis. Cambridge University Press, Cambridge, United Kingdom.
2. **Sylwester AW, Mitchell BL, Edgar JB, Taormina C, Pelte C, Ruchti F, Sleath PR, Grabstein KH, Hosken NA, Kern F, Nelson JA, Picker LJ.** 2005. Broadly targeted human cytomegalovirus-specific CD4+ and CD8+ T cells dominate the memory compartments of exposed subjects. J Exp Med **202:**673–685. http://dx.doi.org/10.1084/jem.20050882.
3. **Wang D, Fu TM.** 2014. Progress on human cytomegalovirus vaccines for prevention of congenital infection and disease. Curr Opin Virol **6:**13–23. http://dx.doi.org/10.1016/j.coviro.2014.02.004.
4. **Reddehase MJ.** 2000. The immunogenicity of human and murine cytomegaloviruses. Curr Opin Immunol **12:**390–396. http://dx.doi.org/10.1016/S0952-7915(00)00106-0.
5. **Brune W.** 2011. Inhibition of programmed cell death by cytomegaloviruses. Virus Res **157:**144–150. http://dx.doi.org/10.1016/j.virusres.2010.10.012.
6. **Jarvis MA, Nelson JA.** 2002. Human cytomegalovirus persistence and latency in endothelial cells and macrophages. Curr Opin Microbiol **5:**403–407. http://dx.doi.org/10.1016/S1369-5274(02)00334-X.
7. **Brune W, Hengel H, Koszinowski UH.** 2001. A mouse model for cytomegalovirus infection. Curr Protoc Immunol **19:**Unit 19.7. http://dx.doi.org/10.1002/0471142735.im1907s43.
8. **Wu CA, Paveglio SA, Lingenheld EG, Zhu L, Lefrançois L, Puddington L.** 2011. Transmission of murine cytomegalovirus in breast milk: a model of natural infection in neonates. J Virol **85:**5115–5124. http://dx.doi.org/10.1128/JVI.01934-10.
9. **Stahl FR, Heller K, Halle S, Keyser KA, Busche A, Marquardt A, Wagner K, Boelter J, Bischoff Y, Kremmer E, Arens R, Messerle M, Förster R.** 2013. Nodular inflammatory foci are sites of T cell priming and control of murine cytomegalovirus infection in the neonatal lung. PLoS Pathog **9:**e1003828. http://dx.doi.org/10.1371/journal.ppat.1003828.
10. **Tan CS, Frederico B, Stevenson PG.** 2014. Herpesvirus delivery to the murine respiratory tract. J Virol Methods **206:**105–114. http://dx.doi.org/10.1016/j.jviromet.2014.06.003.
11. **Hsu KM, Pratt JR, Akers WJ, Achilefu SI, Yokoyama WM.** 2009. Murine cytomegalovirus displays selective infection of cells within hours after systemic administration. J Gen Virol **90:**33–43. http://dx.doi.org/10.1099/vir.0.006668-0.
12. **Collins TM, Quirk MR, Jordan MC.** 1994. Biphasic viremia and viral gene expression in leukocytes during acute cytomegalovirus infection of mice. J Virol **68:**6305–6311.
13. **Stoddart CA, Cardin RD, Boname JM, Manning WC, Abenes GB, Mocarski ES.** 1994. Peripheral blood mononuclear phagocytes mediate dissemination of murine cytomegalovirus. J Virol **68:**6243–6253.
14. **Sacher T, Podlech J, Mohr CA, Jordan S, Ruzsics Z, Reddehase MJ, Koszinowski UH.** 2008. The major virus-producing cell type during murine cytomegalovirus infection, the hepatocyte, is not the source of virus dissemination in the host. Cell Host Microbe **3:**263–272. http://dx.doi.org/10.1016/j.chom.2008.02.014.
15. **Constien R, Forde A, Liliensiek B, Gröne HJ, Nawroth P, Hämmerling G, Arnold B.** 2001. Characterization of a novel EGFP reporter mouse to monitor Cre recombination as demonstrated by a Tie2 Cre mouse line. Genesis **30:**36–44. http://dx.doi.org/10.1002/gene.1030.
16. **Daley-Bauer LP, Roback LJ, Wynn GM, Mocarski ES.** 2014. Cytomegalovirus hijacks CX3CR1(hi) patrolling monocytes as immune-privileged vehicles for dissemination in mice. Cell Host Microbe **15:**351–362. http://dx.doi.org/10.1016/j.chom.2014.02.002.
17. **Gray EE, Cyster JG.** 2012. Lymph node macrophages. J Innate Immun **4:**424–436. http://dx.doi.org/10.1159/000337007.
18. **Hickman HD, Takeda K, Skon CN, Murray FR, Hensley SE, Loomis J, Barber GN, Bennink JR, Yewdell JW.** 2008. Direct priming of antiviral CD8+ T cells in the peripheral interfollicular region of lymph nodes. Nat Immunol **9:**155–165. http://dx.doi.org/10.1038/ni1557.
19. **Iannacone M, Moseman EA, Tonti E, Bosurgi L, Junt T, Henrickson SE, Whelan SP, Guidotti LG, von Andrian UH.** 2010. Subcapsular sinus macrophages prevent CNS invasion on peripheral infection with a neurotropic virus. Nature **465:**1079–1083. http://dx.doi.org/10.1038/nature09118.
20. **Winkelmann ER, Widman DG, Xia J, Johnson AJ, van Rooijen N, Mason PW, Bourne N, Milligan GN.** 2014. Subcapsular sinus macrophages limit dissemination of West Nile virus particles after inoculation but are not essential for the development of West Nile virus-specific T cell responses. Virology **450–451:**278–289. http://dx.doi.org/10.1016/j.virol.2013.12.021.
21. **Caton ML, Smith-Raska MR, Reizis B.** 2007. Notch-RBP-J signaling controls the homeostasis of CD8$^-$ dendritic cells in the spleen. J Exp Med **204:**1653–1664. http://dx.doi.org/10.1084/jem.20062648.
22. **Asano K, Nabeyama A, Miyake Y, Qiu CH, Kurita A, Tomura M, Kanagawa O, Fujii S, Tanaka M.** 2011. CD169-positive macrophages dominate antitumor immunity by crosspresenting dead cell-associated antigens. Immunity **34:**85–95. http://dx.doi.org/10.1016/j.immuni.2010.12.011.
23. **Van Rooijen N, Sanders A.** 1994. Liposome mediated depletion of macrophages: mechanism of action, preparation of liposomes and applications. J Immunol Methods **174:**83–93. http://dx.doi.org/10.1016/0022-1759(94)90012-4.
24. **Lawler C, Milho R, May JS, Stevenson PG.** 2015. Rhadinovirus host entry by co-operative infection. PLoS Pathog **11:**e1004761. http://dx.doi.org/10.1371/journal.ppat.1004761.
25. **Sell S, Dietz M, Schneider A, Holtappels R, Mach M, Winkler TH.** 2015. Control of murine cytomegalovirus infection by γδ T cells. PLoS Pathog **11:**e1004481. http://dx.doi.org/10.1371/journal.ppat.1004481.
26. **Snyder CM, Allan JE, Bonnett EL, Doom CM, Hill AB.** 2010. Cross-presentation of a spread-defective MCMV is sufficient to prime the majority of virus-specific CD8+ T cells. PLoS One **5:**e9681. http://dx.doi.org/10.1371/journal.pone.0009681.
27. **Davis-Poynter NJ, Lynch DM, Vally H, Shellam GR, Rawlinson WD, Barrell BG, Farrell HE.** 1997. Identification and characterization of a G protein-coupled receptor homolog encoded by murine cytomegalovirus. J Virol **71:**1521–1529.
28. **Jordan S, Krause J, Prager A, Mitrovic M, Jonjic S, Koszinowski UH, Adler B.** 2011. Virus progeny of murine cytomegalovirus bacterial artificial chromosome pSM3fr show reduced growth in salivary glands due to a fixed mutation of MCK-2. J Virol **85:**10346–10353. http://dx.doi.org/10.1128/JVI.00545-11.
29. **Smith LM, McWhorter AR, Masters LL, Shellam GR, Redwood AJ.** 2008. Laboratory strains of murine cytomegalovirus are genetically similar to but phenotypically distinct from wild strains of virus. J Virol **82:**6689–6696. http://dx.doi.org/10.1128/JVI.00160-08.
30. **Brown MG, Dokun AO, Heusel JW, Smith HR, Beckman DL, Blattenberger EA, Dubbelde CE, Stone LR, Scalzo AA, Yokoyama WM.** 2001. Vital involvement of a natural killer cell activation receptor in resistance to viral infection. Science **292:**934–937. http://dx.doi.org/10.1126/science.1060042.
31. **Smith HR, Heusel JW, Mehta IK, Kim S, Dorner BG, Naidenko OV, Iizuka K, Furukawa H, Beckman DL, Pingel JT, Scalzo AA, Fremont DH, Yokoyama WM.** 2002. Recognition of a virus-encoded ligand by a natural killer cell activation receptor. Proc Natl Acad Sci U S A **99:**8826–8831. http://dx.doi.org/10.1073/pnas.092258599.
32. **Taylor PR, Martinez-Pomares L, Stacey M, Lin HH, Brown GD, Gordon S.** 2005. Macrophage receptors and immune recognition. Annu Rev Immunol **23:**901–944. http://dx.doi.org/10.1146/annurev.immunol.23.021704.115816.
33. **Rosa GT, Gillet L, Smith CM, de Lima BD, Stevenson PG.** 2007. IgG fc receptors provide an alternative infection route for murine gammaherpesvirus-68. PLoS One **2:**e560. http://dx.doi.org/10.1371/journal.pone.0000560.
34. **Xu J, Scalzo AA, Lyons PA, Farrell HE, Rawlinson WD, Shellam GR.** 1994. Identification, sequencing and expression of the glycoprotein L gene of murine cytomegalovirus. J Gen Virol **75:**3235–3240. http://dx.doi.org/10.1099/0022-1317-75-11-3235.
35. **Nikbakht N, Shen S, Manser T.** 2013. Cutting edge: macrophages are

required for localization of antigen-activated B cells to the follicular perimeter and the subsequent germinal center response. J Immunol **190:** 4923–4927. http://dx.doi.org/10.4049/jimmunol.1300350.

36. **Probst HC, Tschannen K, Odermatt B, Schwendener R, Zinkernagel RM, Van Den Broek M.** 2005. Histological analysis of CD11c-DTR/GFP mice after in vivo depletion of dendritic cells. Clin Exp Immunol **141:**398–404. http://dx.doi.org/10.1111/j.1365-2249.2005.02868.x.
37. **Frederico B, Chao B, May JS, Belz GT, Stevenson PG.** 2014. A murid gamma-herpesvirus exploits normal splenic immune communication routes for systemic spread. Cell Host Microbe **15:**457–470. http://dx.doi.org/10.1016/j.chom.2014.03.010.
38. **Sinclair J, Reeves M.** 2014. The intimate relationship between human cytomegalovirus and the dendritic cell lineage. Front Microbiol **5:**389. http://dx.doi.org/10.3389/fmicb.2014.00389.
39. **Fenner F.** 2000. Adventures with poxviruses of vertebrates. FEMS Microbiol Rev **24:**123–133. http://dx.doi.org/10.1111/j.1574-6976.2000.tb00536.x.
40. **Volkman A, Gowans JL.** 1965. The origin of macrophages from bone marrow in the rat. Br J Exp Pathol **46:**62–70.
41. **Gaspar M, May JS, Sukla S, Frederico B, Gill MB, Smith CM, Belz GT, Stevenson PG.** 2011. Murid herpesvirus-4 exploits dendritic cells to infect B cells. PLoS Pathog **7:**e1002346. http://dx.doi.org/10.1371/journal.ppat.1002346.
42. **Sunil-Chandra NP, Efstathiou S, Nash AA.** 1992. Murine gammaherpesvirus 68 establishes a latent infection in mouse B lymphocytes in vivo. J Gen Virol **73:**3275–3279. http://dx.doi.org/10.1099/0022-1317-73-12-3275.
43. **Hamano S, Yoshida H, Takimoto H, Sonoda K, Osada K, He X, Minamishima Y, Kimura G, Nomoto K.** 1998. Role of macrophages in acute murine cytomegalovirus infection. Microbiol Immunol **42:**607–616. http://dx.doi.org/10.1111/j.1348-0421.1998.tb02331.x.
44. **Hanson LK, Slater JS, Karabekian Z, Virgin HW, Biron CA, Ruzek MC, van Rooijen N, Ciavarra RP, Stenberg RM, Campbell AE.** 1999. Replication of murine cytomegalovirus in differentiated macrophages as a determinant of viral pathogenesis. J Virol **73:**5970–5980.
45. **Junt T, Moseman EA, Iannacone M, Massberg S, Lang PA, Boes M, Fink K, Henrickson SE, Shayakhmetov DM, Di Paolo NC, van Rooijen N, Mempel TR, Whelan SP, von Andrian UH.** 2007. Subcapsular sinus macrophages in lymph nodes clear lymph-borne viruses and present them to antiviral B cells. Nature **450:**110–114. http://dx.doi.org/10.1038/nature06287.
46. **Garcia Z, Lemaître F, van Rooijen N, Albert ML, Levy Y, Schwartz O, Bousso P.** 2012. Subcapsular sinus macrophages promote NK cell accumulation and activation in response to lymph-borne viral particles. Blood **120:**4744–4750. http://dx.doi.org/10.1182/blood-2012-02-408179.
47. **Mitrović M, Arapović J, Traven L, Krmpotić A, Jonjić S.** 2012. Innate immunity regulates adaptive immune response: lessons learned from studying the interplay between NK and CD8+ T cells during MCMV infection. Med Microbiol Immunol **201:**487–495. http://dx.doi.org/10.1007/s00430-012-0263-0.
48. **Sandberg K, Eloranta ML, Campbell IL.** 1994. Expression of alpha/beta interferons (IFN-alpha/beta) and their relationship to IFN-alpha/beta-induced genes in lymphocytic choriomeningitis. J Virol **68:**7358–7366.
49. **Chong KT, Gresser I, Mims CA.** 1983. Interferon as a defence mechanism in mouse cytomegalovirus infection. J Gen Virol **64:**461–464. http://dx.doi.org/10.1099/0022-1317-64-2-461.
50. **Bosio E, Beilharz MW, Watson MW, Lawson CM.** 1999. Efficacy of low-dose oral use of type I interferon in cytomegalovirus infections in vivo. J Interferon Cytokine Res **19:**869–876. http://dx.doi.org/10.1089/107999099313389.
51. **Salazar-Mather TP, Lewis CA, Biron CA.** 2002. Type I interferons regulate inflammatory cell trafficking and macrophage inflammatory protein 1alpha delivery to the liver. J Clin Investig **110:**321–330. http://dx.doi.org/10.1172/JCI15376.
52. **Honke N, Shaabani N, Cadeddu G, Sorg UR, Zhang DE, Trilling M, Klingel K, Sauter M, Kandolf R, Gailus N, van Rooijen N, Burkart C, Baldus SE, Grusdat M, Löhning M, Hengel H, Pfeffer K, Tanaka M, Häussinger D, Recher M, Lang PA, Lang KS.** 2012. Enforced viral replication activates adaptive immunity and is essential for the control of a cytopathic virus. Nat Immunol **13:**51–57. http://dx.doi.org/10.1038/ni.2169.
53. **Zhang X, Bogunovic D, Payelle-Brogard B, Francois-Newton V, Speer SD, Yuan C, Volpi S, Li Z, Sanal O, Mansouri D, Tezcan I, Rice GI, Chen C, Mansouri N, Mahdaviani SA, Itan Y, Boisson B, Okada S, Zeng L, Wang X, Jiang H, Liu W, Han T, Liu D, Ma T, Wang B, Liu M, Liu JY, Wang QK, Yalnizoglu D, Radoshevich L, Uzé G, Gros P, Rozenberg F, Zhang SY, Jouanguy E, Bustamante J, García-Sastre A, Abel L, Lebon P, Notarangelo LD, Crow YJ, Boisson-Dupuis S, Casanova JL, Pellegrini S.** 2015. Human intracellular ISG15 prevents interferon-α/β over-amplification and auto-inflammation. Nature **517:**89–93. http://dx.doi.org/10.1038/nature13801.
54. **Braun A, Worbs T, Moschovakis GL, Halle S, Hoffmann K, Bölter J, Münk A, Förster R.** 2011. Afferent lymph-derived T cells and DCs use different chemokine receptor CCR7-dependent routes for entry into the lymph node and intranodal migration. Nat Immunol **12:**879–887. http://dx.doi.org/10.1038/ni.2085.